Lattice thermal conductivity of deformed and annealed aluminum alloys in the temperature range 1.3–60 K†

R. W. Klaffky,* N. S. Mohan, and D. H. Damon
Department of Physics and Institute of Materials Science, University of Connecticut, Storrs, Connecticut 06268
(Received 19 September 1974)

The thermal conductivity of several aluminum-magnesium and other aluminum alloys has been measured between 1.3 and 60 K in order to study point defects and dislocations in these metals. The measured thermal conductivity is separated into electronic and lattice components. The lattice thermal conductivity of each sample is analyzed in terms of the scattering of phonons by electrons, dislocations, and point defects. The measured lattice thermal conductivity of the well-annealed specimens at 10 K is in good agreement with a theoretical estimate of the effect of phonon scattering by electrons. Samples deformed by swaging have a larger lattice thermal resistivity which is shown to be due to dislocations in concentrations as large as 2×10^{11} cm^{-2} in the heavily deformed samples. The dislocation densities deduced from the lattice thermal conductivities are compared to estimates from electron microscopy. The rate of phonon scattering by point defects is shown to scale with magnesium concentrations in the aluminum-magnesium alloys; its magnitude is consistent with the local lattice distortion that accompanies the introduction of a magnesium atom into the aluminum lattice.

I. INTRODUCTION

The lattice thermal conductivity of a crystal is sensitive to the type and concentrations of the defects it contains. As discussed by Klemens[1] this is a result of the temperature dependence of the *dominant* phonon wavelength which increases from a value of the order of the lattice parameter at high temperatures to values of hundreds of angstroms at liquid-helium temperatures. Consequently, the scattering of phonons by defects, and hence the lattice thermal conductivity, depends on the size and geometrical shapes of the lattice defects. This paper deals with the effects of dislocations and point defects on the lattice thermal conductivity of aluminum-magnesium alloys between 1.3 and 60 K. The samples, which have concentrations of 3- to 7-at.% Mg, were measured in swaged and annealed states. Previous measurements have been reported for commercial aluminum alloys[2] and for a 1-at.% aluminum-magnesium alloy during age hardening.[3] This work presents a systematic study of the effect of magnesium concentration and cold work on the lattice thermal conductivity of α-phase aluminum-magnesium.

The measured thermal conductivity consists of a lattice and an electronic component. Since the effects of different types of defects are not distinguished by the temperature dependence of the electronic thermal conductivity,[1] this component must be subtracted away in order to obtain the more interesting lattice thermal conductivity. If the scattering of electrons by solute atoms dominates then the electronic thermal conductivity is easily obtained from measurements of the electrical resistivity by using the Wiedemann-Franz law. In another publication we have shown that the measured thermal conductivity of these aluminum alloys can be readily separated into lattice and electronic components below about 25 K.[4]

For each sample the resulting lattice thermal conductivity K_g approaches a T^2 dependence below 10 K where only electron-phonon scattering and dislocation-phonon scattering are important. Above 10 K, K_g varies less rapidly than T^2 because of the point-defect scattering that results from our high solute concentrations. The maximum in K_g occurs at approximately 35 K. By fitting theoretical formulas to the experimental data below 25 K we separate the scattering into contributions from the electron-phonon, dislocation-phonon, and point-defect–phonon interactions. From the scattering strengths of these interactions we estimate the dislocation densities for the heavily swaged samples and the lattice distortion caused by a magnesium atom. The lattice thermal conductivity of dislocation-free aluminum is found to be in good agreement with theory. To determine whether our heat treatments were properly removing dislocations, we have examined several swaged and annealed samples with an electron microscope. The number of dislocations remaining after a given heat treatment is correlated with the corresponding value of the lattice thermal conductivity.

II. EXPERIMENTAL METHOD

A. Sample preparation

With the exception of two commercial aluminum alloys of ASTM numbers 2024 and 5052, all samples were prepared in this laboratory. An induction furnace was used to melt aluminum in a graphite crucible over which a steady stream of argon or helium was passed to prevent oxidation. After stirring magnesium into the molten aluminum, the resulting alloy was poured into a 110 electrolytic

TABLE I. Characteristics of the measured aluminum alloys.

Sample	Composition	Mechanical/heat treatment (Unless otherwise stated, samples were water quenched after annealing.)	ρ_0(4.2 K) ($\mu\Omega$ cm)	K_g(10 K) (W m^{-1} K^{-1})
1	5052[a]	swaged $\frac{1}{2}$ to $\frac{1}{8}$ in.	2.017	0.41
1a		annealed at 400 °C for 72 h	1.894	0.62
1b		annealed at 606 °C for 24 h; slow cooled in furnace to 400 °C (50 °C/h)	1.977	0.75
2	5% Mg[b]	swaged $\frac{1}{4}$ to $\frac{1}{8}$ in.	1.980	...
2a		annealed at 200 °C for 96 h, further at 350 °C for 72 h and further at 465 °C for 8$\frac{1}{2}$ h	1.842	0.64
2b		annealed further at 500 °C for 20 h; slow cooled in furnace (50 °C/h) to 20 °C	1.828	0.60
3	5% Mg[b]	swaged $\frac{1}{4}$ to $\frac{1}{8}$ in.	2.045	0.40
3a		annealed at 570 °C for 16 h; kept at 400 °C for 24 h	1.869	0.63
3b		annealed at 603 °C for 17 h; slow cooled in furnace (1 °C/min) to 270 °C	1.862	0.81
4	7% Mg[b]	swaged $\frac{3}{8}$ to $\frac{1}{8}$ in.; annealed at 603 °C for 16 h; slow cooled in furnace (1 °C/min) to 435 °C	2.812	0.79
5	7% Mg[b]	swaged $\frac{3}{8}$ to $\frac{1}{8}$ in.	2.744	0.53
6	7% Mg[b]	swaged $\frac{3}{16}$ to $\frac{1}{8}$ in.	2.521	0.52
6a		annealed at 400 °C for 25 h; air quenched	2.424	0.62
7	7% Mg[b]	swaged $\frac{3}{8}$ to $\frac{1}{8}$ in.; annealed at 200 °C for 96 h, further at 350 °C for 72 h, further at 465 °C for 8$\frac{1}{2}$ h; further at 575 °C for 10 h; kept at 400 °C for 15 h	2.359	0.64
8	2024[a]	swaged $\frac{1}{4}$ to $\frac{1}{8}$ in.	3.331	0.35
9	5052[a]	swaged $\frac{1}{2}$ to $\frac{1}{8}$ in.; annealed at 609 °C for 24 h; slow cooled to 567 °C (1 °C/min); kept at 567 °C for 24 h	2.044	0.67

[a]Commercial alloys specified by their ASTM numbers.

[b]Composition of the starting material (at.%).

copper mold. The castings were then homogenized at 425 °C before being swaged at room temperature to $\frac{1}{8}$-in.-diam samples. The 99.99% aluminum was supplied by the Aluminum Corporation of America, Pittsburgh, Pa. and the 99.99% magnesium by Research Organic/Inorganic Chemical Corp., Sun Valley, Calif. A resistivity profile of several samples indicated homogeneity over their lengths. Table I lists the samples measured in this experiment, their nominal composition (i.e., the composition of the starting material), mechanical and heat treatments, and residual resistivities. Initially, the samples were annealed in a vacuum but this led to a magnesium loss of as much as 5%, which was reflected in corresponding changes in the residual resistivity and sample weight. To prevent magnesium loss, the technique of Chaterjee and Entwistle[5] was employed, in which the samples were first anodized and then annealed in a CO_2 environment. With this technique it was possible to anneal at temperatures above 600 °C without weight loss.

In this paper we use the residual resistivity increment of 0.46 Ω cm/at.%-Mg recommended by Fickett[6] in conjunction with the residual resistivities listed in Table I to estimate the magnesium concentrations of each sample. The magnesium concentrations calculated in this manner indicate that approximately 1-at.% Mg was lost during casting. This is not an unreasonable loss because magnesium has a considerably higher volatility than aluminum.

B. Electron microscopy

Slices of 0.030-in. thickness were spark cut from the middle of several swaged and annealed samples whose thermal conductivity had been measured. A solution of HCl (200 cm^3), NiCl (5 g), and H_2O (300 cm^3) was used to thin each slice to a thickness of about 0.010 in. A Fischione model No. 110 electropolisher further thinned the slice by passing jets of an 80%-methyl-alcohol–20%-perchloric-acid electrolyte perpendicular to both sides of the slice until a small hole appeared. The electrolyte was maintained at – 20 °C by a Lauda Model No. IC-6 immersion cooler. The slice was then rinsed in alcohol and distilled water and mounted in a Philips EM300 electron microscope for observation. Typical magnifications of 20 000× to 50 000× were used to observe the dislocations.

C. Measurement techniques

The experimental measurements between 4 and 60 K were made with a Swenson cryostat in which cold helium gas was used to cool a thermally isolated sample platform suspended in a vacuum chamber. The cryostat design has been described in a previous paper.[7] The temperature of the platform was controlled by an Artronix Model No. 5301 temperature controller using a germanium resistor as a sensor below 25 K and a platinum resistor as a sensor from 25 to 70 K. For measurements from 1.3 to 4 K a conventional cryostat was utilized in which the sample platform was in good thermal contact with the helium bath. The temperature of the bath was regulated by pumping on the helium using a Walker pressure regulator.

The total thermal conductivity K was determined by the steady-state method from the relationship

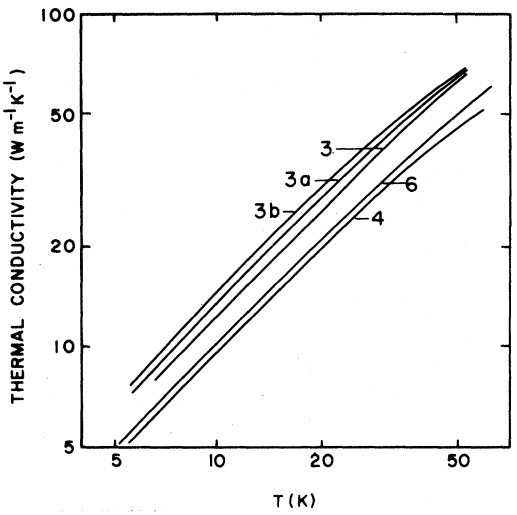

FIG. 1. Measured values of the thermal conductivity of three aluminum-magnesium alloys vs absolute temperature T. This figure shows the effects of solute concentration, cold work and heat treatment. (See text and Table I.)

$K = QL/A\Delta T$, where Q was the steady heat flow through the sample, A was the cross-sectional area, and L and ΔT were the distance and temperature difference between two thermometers, respectively. The cold end of the sample was clamped to the platform. A 10-K Evanohm heater coil, which was clamped to the hot end of the sample, established the heat flow Q. The temperature difference ΔT was measured by calibrated Cryocal germanium resistors, which were mounted in aluminum clamps spaced 2 in. apart. In order to ensure temperature stability at each measurement, both the cold and hot thermometer voltages were monitored on a chart recorder for times up to 1 h. For each platform temperature, the temperature difference ΔT was measured with no heater power in order to correct for extraneous heat sources. A copper shield in good thermal contact with the platform surrounded the sample and thereby reduced radiation loss from the sample to the helium bath. The temperatures of the heater and the sample platform were measured by germanium resistors to correct for radiation losses to the shield. Corrections for the Joule heating in the heater current leads were also made.

The accuracy of the thermal conductivity measurements was limited primarily by the absolute accuracy of the thermometer calibration (1%), and by the accuracy of the sample geometry factor L/A (2%). The same set of clamps served as potential probes for the electrical resistivity measurements and as thermometer mounts in the thermal conductivity measurements. Since the sample geometry factor was identical for both measurements, the accuracy of the lattice thermal conductivity was also 2%. The accuracy of the electrical resistance measurements was 0.1% and, therefore, did not introduce further uncertainty into the calculation of the lattice thermal conductivities. The precision of the thermal-conductance measurements ($Q/\Delta T$) was 0.1%; this is reflected in a scatter of about ±2% in the lattice thermal-conductivity values shown in Figs. 4 and 5.

III. EXPERIMENTAL RESULTS

A. Thermal conductivity

Figure 1 shows the results of the measurements of the thermal conductivity of several aluminum-magnesium alloys with concentrations ranging from 4 to 6 at.% (the sample concentrations are calculated from the residual resistivity of each sample, as discussed above). The values measured between 4 and 1.2 K are not shown here. For clarity, points showing the measured values have been omitted on this and on the following figure because they show no scatter about the drawn curves.

The magnitude of the thermal conductivity is determined primarily by the solute concentration because the electronic thermal conductivity constitutes the major part of the total. As a result, the effects of changes in the lattice thermal conductivity resulting from variations in the dislocation density are of only secondary importance. For example, the thermal conductivities of samples 6 (5.5-at.% Mg) and 4 (6.1-at.% Mg) are smaller than the thermal conductivity of sample 3 (4.5-at.% Mg) because of the smaller electronic thermal conductivities associated with their higher electrical resistivities. In addition, sample 4 has a lower thermal conductivity than sample 6 even though sample 4 was measured in a well-annealed state and sample 6 in a heavily deformed state. In fact, as will be shown below, the *lattice* thermal conductivity of sample 4 is about two times that of sample 6.

The curve labeled 3 shows the measured values of the thermal conductivity of this sample in a heavily deformed state; the curve 3a after annealing at 570 °C and 3b after annealing at over 600 °C. Part of the increase resulting from annealing at 570 °C was due to an increase in its electronic thermal conductivity, almost certainly caused by a loss of magnesium (see Table I). In the second annealing the anodizing technique was used and little, if any, magnesium was lost; the increase observed here is due entirely to an increase in the lattice thermal conductivity.

We have also measured the thermal conductivity of a commercial 2024-T351 alloy and several commercial 5052 alloys, as shown in Fig. 2. The 2024 alloy (sample 8) has the lowest thermal conductivity corresponding to its relatively large residual resistivity of 3.33 $\mu\Omega$ cm. This sample was swaged

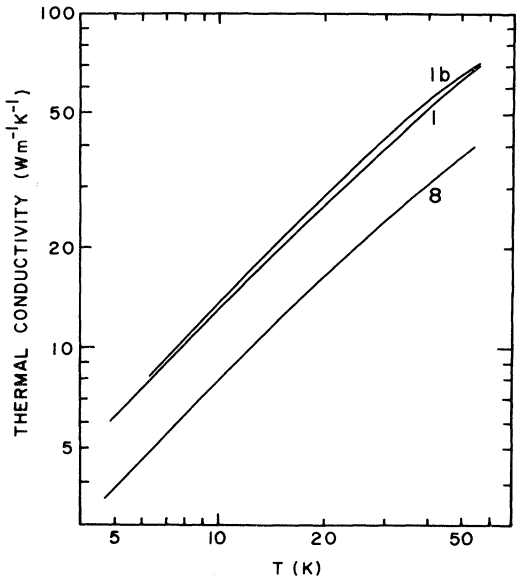

FIG. 2. Measured values of the thermal conductivity of two commercial aluminum alloys vs absolute temperature. (See Table I.)

from $\frac{1}{4}$ to $\frac{1}{8}$ in. in our laboratory. Since our heat treatments of the 2024 alloy always produced large changes in its residual resistivity, we did not measure the thermal conductivity of this specimen in an annealed state. Similar difficulties were encountered by Hust and Sparks[8] who measured the electrical and thermal conductivity of a 2024-T86 alloy with a residual resistivity that changed upon annealing at 427 °C. The 5052 alloy (sample 1) has been measured in the swaged state as well as the fully annealed state (sample 1b). Sample 1b has a larger thermal conductivity because there was a magnesium loss upon annealing at 603 °C and an increase in the lattice thermal conductivity corresponding to a reduction in the dislocation density.

B. Electrical resistivity

The electrical resistivity has been measured from 4 to 60 K for each sample. An accurate value of the residual resistivity is determined from the measurement of ρ at 4 K. The electrical resistivity can be expressed as

$$\rho = \rho_0 + \rho_i + \Delta\rho \,, \tag{1}$$

where ρ_i is the ideal resistivity of pure aluminum ($\rho_0 = 0$) and $\Delta\rho$ is the deviation from Matthiessen's rule. The ideal resistivity is calculated using the Grüneisen-Bloch formula with a Debye temperature of 400 K and $\rho(273.15\ \mathrm{K}) = 2.42\ \mu\Omega\,\mathrm{cm}$. According to Fickett,[6] this gives the best fit to the available resistivity data for pure aluminum in the temperature range of interest to us. A full description of the variation of $\Delta\rho$ with solute concentration and cold work will be published elsewhere.[9]

C. Separation of the lattice and electronic thermal conductivities

The total thermal conductivity K consists of an electronic component K_e and a lattice component K_g such that

$$K = K_e + K_g \,. \tag{2}$$

The electronic thermal resistivity K_e^{-1} is the sum of the thermal resistivity due to the scattering of electrons by defects W_0, the thermal resistivity due to the scattering of electrons by phonons W_i, and a term ΔW which represents any deviation from strict additivity of the scattering rates. Thus,

$$K_e^{-1} = W_0 + W_i + \Delta W \,. \tag{3}$$

This is the thermal analog to Eq. (1). There are no universal equations relating ρ_i and W_i or $\Delta\rho$ and ΔW since any such relationships will depend on the relative strengths of the scattering mechanisms and on the shape of the Fermi surface. Consequently one cannot expect to calculate K_e from measurements of ρ under all circumstances. However, if impurity scattering dominates then W_i, ΔW, ρ_i, and $\Delta\rho$ are all negligible and K_e^{-1} is given by the Wiedemann-Franz law, namely,

$$K_e^{-1} = W_0 = \rho_0 / LT \,, \tag{4}$$

where $L = 2.45 \times 10^{-8}\ \mathrm{V^2K^{-2}}$ is the Lorenz number. This will certainly be true at the lowest temperatures. Further, if in this same range of temperatures the phonons are scattered only by electrons and sessile dislocations then theory[1] shows that K_g will vary as T^2. Therefore, K/T should be a linear function of T since

$$K/T = K_e/T + K_g/T = L/\rho_0 + \beta T \,, \tag{5}$$

where β is a constant. We have found this to be the case for all of our alloys over the temperature range 1.3–10 K. Figure 3 shows such a plot for two of the samples; it is clear that Eq. (5) accurately represents these results. We note that the measurements above and below 4.2 K were made on different apparatuses with different thermometers. The excellent agreement between these results is another indication of the high accuracy of these measurements. As is evident in these plots, K_g is difficult to measure at temperatures below 4 K since it represents only a few percent of the total conductivity. For this reason the analysis of the lattice thermal conductivity will be based on measurements above 4 K.

In another publication[4] we have discussed in detail the calculation of K_e from Eq. (3) for our aluminum alloys. For W_i the values of the thermal conductivity of pure aluminum measured by Fenton,

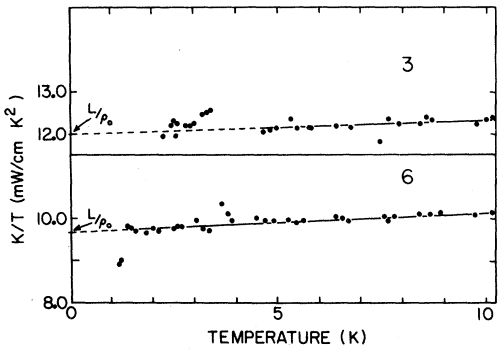

FIG. 3. Measured values of the thermal conductivity divided by temperature for two aluminum magnesium alloys (See Table I) plotted against temperature. This figure shows the separation of the total thermal conductivity into an electronic thermal conductivity $K_e = LT/\rho_0$ and a lattice thermal conductivity varying as T^2.

Rogers, and Woods[10] were combined with the recommendations of the Thermophysical Properties Research Center.[11]

These values of W_i are described by the empirical relations

$$W_i = (1.09)\times 10^{-6} T^{2.87}, \quad T > 30\ \text{K}, \qquad W_i = (2.80)\times 10^{-5} T^{1.9}, \quad T < 30\ \text{K}. \tag{6}$$

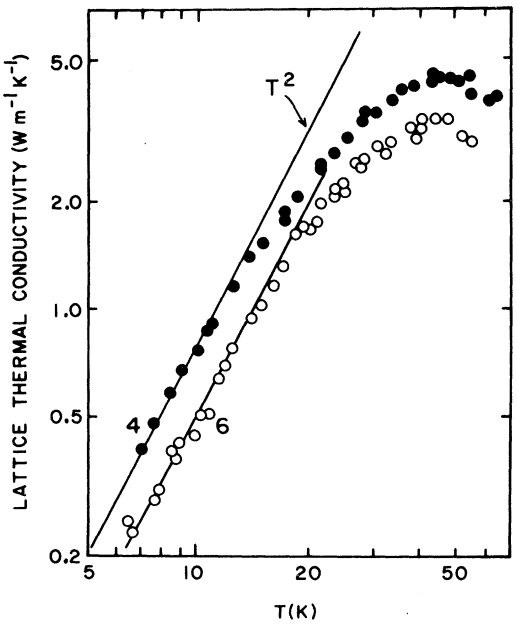

FIG. 4. Lattice thermal conductivities of two aluminum-magnesium alloys vs absolute temperature T. The lattice thermal conductivity K_g is obtained from the measured total thermal conductivity K by subtracting the electronic thermal conductivity K_e, i.e., $K_g = K - K_e$ (see text for a description of this subtraction).

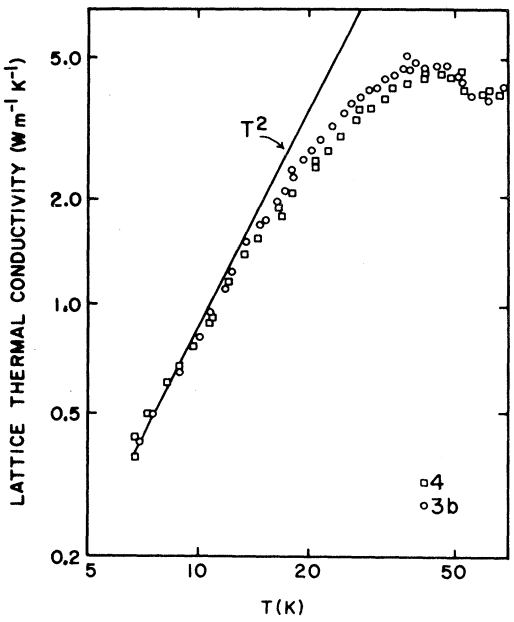

FIG. 5. Lattice thermal conductivities ($K_g = K - K_e$) of two well-annealed aluminum-magnesium alloys vs absolute temperature. At the lowest and highest temperatures the lattice thermal conductivities are nearly the same. The difference at intermediate temperatures is due to stronger point defect scattering resulting from a higher concentration of magnesium atoms for sample 4.

The ΔW term can be calculated from measured values of the deviations from Matthiessen's rule by assuming that a Wiedemann-Franz law relates ΔW to $\Delta\rho$, i.e.,

$$\Delta W = \Delta\rho/LT. \tag{7}$$

The values of the lattice thermal conductivity resulting from this calculation are shown in Figs. 4–6 for several of our samples. The lattice thermal conductivities approach a T^2 dependence at the lowest temperatures, where electron-phonon and dislocation-phonon scattering dominate. The heavily swaged samples have a significantly lower lattice thermal conductivity than the well-annealed samples as a result of their large dislocation densities. The values of the lattice thermal conductivity at 10 K, K_g(10 K), range from 0.4 W m^{-1} K^{-1} for the heavily swaged samples to 0.8 W m^{-1} K^{-1} for the samples annealed above 600 °C, as shown in Table I. Electron micrographs indicate that the heavily swaged samples have 1-μm grains which is characteristic of heavily cold-worked aluminum.[12] After annealing sample 2b at 500 °C a relatively high density of dislocations was observed with the electron microscope even though the grain size had increased to several mm. This result is consistent with the K_g(10 K) values of approximately 0.6 W m^{-1} K^{-1} for sample 2b and other samples annealed

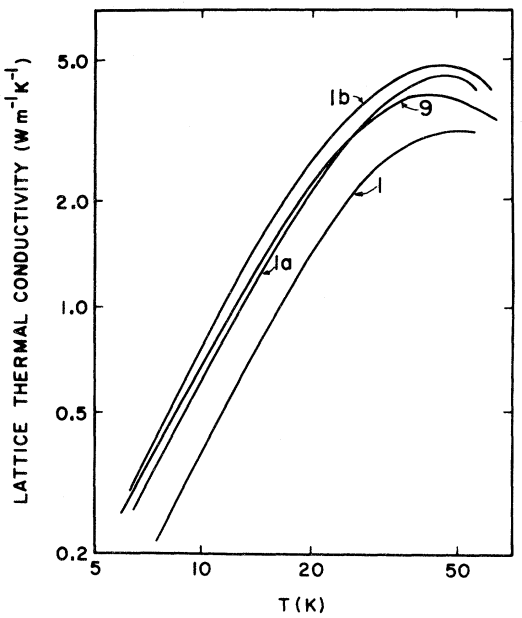

FIG. 6. Lattice thermal conductivities of swaged 5052 aluminum alloys after various heat treatments (see text and Table I) vs absolute temperature.

between 400 and 575 °C as shown in Table I. It was necessary to anneal at temperatures above 600 °C to reduce the dislocation density to less than 10^8 lines/cm^2, corresponding to K_g(10 K) values of about 0.8 W m^{-1}K^{-1}. The value of 10^8 cm^{-2} is an upper bound as it was based on the observation of large areas of dislocation-free regions in our electron micrographs with only a few isolated dislocation lines between these regions.

We feel that the value of 0.8 W m^{-1} K^{-1}, which is independent of magnesium concentration, represents the first reliable value for the intrinsic lattice thermal conductivity of well-annealed aluminum. Previous measurements of Powell *et al.*[2] for commercial aluminum alloys annealed at temperatures below 400 °C gave values of K_g(10 K) ranging from 0.9 to 2.5 W m^{-1}K^{-1}. The wide range of their K_g values can perhaps be explained by a 2% scatter in their measurements of the electrical resistance. The value of 60 W m^{-1}K^{-1} for K_g(10 K) recently reported by Täubert *et al.*[3] for a 1-at.% Al-Mg alloy annealed at 450 °C is inexplicable.

Above 10 K, the K_g values depart from a T^2 dependence as point defect scattering becomes important. The effect of the point defect scattering is illustrated in Fig. 5 which displays the K_g values of a well-annealed 4-at.%-Mg sample (sample 3b) and a well-annealed 6-at.%-Mg sample (sample 4) as a function of temperature. The K_g values are the same within experimental error for temperatures below 10 K. As the point defect scattering becomes important at higher temperatures, the lattice thermal conductivity of the 6-at.% sample is reduced relative to the 4-at.% sample. The maxima in K_g occur at approximately 40 K. At temperatures above the maximum, anharmonic interactions become more important than point defect scattering, as reflected by the convergence of the K_g values of the 5- and 6-at.%-Mg samples.

In general the maxima occur between 35 and 45 K for the samples we have measured. The few values measured above the maximum show a temperature variation consistent with a T^{-1} behavior expected for three-phonon U processes.

Qualitatively, these observations are consistent with theoretical expectations and provide some justification for the assumptions we have made in calculating K_e. Before proceeding with a quantitative analysis of the strengths of the various scattering mechanism, we must recognize that (a) W_i need not have exactly the same values for pure aluminum and these alloys, and (b) Eq. (5) is not necessarily correct. The relative importance of each term in Eq. (3) has been carefully analyzed in Ref. 4; there we concluded that K_g can be unambiguously calculated from the Wiedemann-Franz law and W_i below 25 K. To summarize that argument we may simply list the 25-K values of the quantities appearing in Eq. (3) for an aluminum alloy with a residual resistivity of 2×10^{-8} Ω m, $W_0 = 3.27\times10^{-2}$, $W_i = 1.27\times10^{-4}$ and $\Delta W = \Delta\rho/LT = 7.36\times10^{-5}$ m K W^{-1}. From these figures we see that if the calculated value of $W_i + \Delta W$ were to be in error by 50% then, in a typical case, the lattice thermal conductivity at 25 K would be in error by 4%. At lower temperatures the terms W_i and ΔW rapidly become insignificant. Henceforth, we restrict all quantitative analysis of our data to those values measured below 25 K.

Figures 1–6 do not show the results of all our measurements. We have selected only those that most clearly show the effects to be discussed below. To assist those who might wish to use our data directly we have tabulated all the experimental results in a separate report[13] available on request from the authors.

IV. DISCUSSION

To quantitatively describe the lattice thermal conductivity one must determine the relative strengths of phonon scattering by electrons, dislocations, point defects, boundaries, and other phonons via U processes. As discussed in an earlier work[4] there is no reason to believe that an error in the calculation of K_e would cause the temperatures of the maxima in the lattice thermal conductivities to be significantly lower than about 40 K as shown in Figs. 4–6.

If the maxima in the lattice thermal conductivity are indeed near 40 K then the scattering strength

for U processes should be negligible below 25 K, since it decreases exponentially with decreasing temperature. The relative strength of the boundary scattering may be estimated by calculating the phonon mean free path l from the standard formula of kinetic theory $l = 3K_g V_m / C_V v$, where V_m is the molar volume, C_V is the lattice specific heat per mole at constant volume, and v is the velocity of sound. Using a Debye specific heat law with $\Theta = 428$ K and $v = 4.38 \times 10^5$ cm sec^{-1} as an average sound velocity one finds $l = 0.47$ μm at 5 K for the well-annealed samples and about half of this value for the deformed specimens. (In the temperature range where $K_g \sim T^2$ and $C_V \sim T^3$, the mean free path will, of course, vary as T^{-1}.) The diameter of the smallest grains in our heavily deformed alloys was about 1 μm; in the annealed alloys the grains were much larger. Therefore, for the temperature range 5–25 K it seems safe to conclude that there should be no need to include the effects of boundary scattering or U processes.

Using a relaxation time solution to the Boltzmann equation the lattice thermal conductivity[1] can be expressed as

$$K_g = \frac{\hbar^2}{2\pi^2 k T^2 v} \int \frac{e^{\hbar\omega/kT}\, \tau(\omega) \omega^4\, d\omega}{(e^{\hbar\omega/kT} - 1)^2} , \tag{8}$$

where k is Boltzmann's constant, v is the average phonon velocity, and the relaxation time $\tau(\omega)$ is a function of the phonon frequency. Since in the temperature range 5–25 K the phonon scattering rate $1/\tau$ is the sum of contributions due to electrons, dislocations, and point defects, we may write

$$\frac{1}{\tau(\omega)} = \frac{1}{\tau_e} + \frac{1}{\tau_d} + \frac{1}{\tau_{pd}} . \tag{9}$$

N processes can be disregarded because, as will be shown below, the dominant scattering processes (phonon-electron and phonon-dislocation) are only weakly dependent on phonon frequency.

At low temperatures the relaxation rate for electron-phonon scattering can be directly related to the thermal conductivity K_g for a dislocation-free sample[14]

$$\frac{1}{\tau_e} = \frac{(14.4)k^3}{\hbar^2 v} \left(\frac{T^2}{K_g}\right) \omega = C\omega \quad (T \ll \Theta) . \tag{10}$$

The relaxation rate for dislocation-phonon scattering[15] is given by

$$1/\tau_d = 2.3\gamma^2 b^2 N_d \omega = D\omega , \tag{11}$$

where γ is the Grüneisen constant, b is the average length of the Burgers vector for dislocations, and N_d is the dislocation density. The scattering of a phonon by a point defect can be described in terms of any one or all of three effects: (i) the difference in mass ΔM between the solute and solvent atoms, (ii) the introduction of a strain field as the lattice dilates or contracts about the solute, and (iii) the interatomic forces between host and solute atoms are not the same as those between host atoms. We shall ignore the third effect and write for the scattering rate of the phonons by point defects,[1]

$$\frac{1}{\tau_{pd}} = \frac{3a^3 f_0 \omega^4}{\pi v^3} \left[\frac{1}{12}\left(\frac{\Delta M}{M}\right)^2 + 3\gamma^2 \left(\frac{\Delta R}{R}\right)^2\right] = A\omega^4 , \tag{12}$$

where f_0 is the atomic fraction of magnesium atoms and $\Delta R/R$ represents the local strain produced by the introduction of the solute.

When the total relaxation rate $1/\tau(\omega)$ is substituted into the integral expression (8) for K_g, one obtains the expression

$$K_g = \frac{2k^3 T^2}{v\hbar^2} \int_0^{\Theta/T} \frac{x^3 e^x\, dx}{(e^x - 1)^2 [(C+D) + Ax^3 (kT/\hbar)^3]} , \tag{13}$$

where $x = \hbar\omega/kT$ and Θ is the Debye temperature of aluminum. In the limit of low T, the point defect term in the denominator can be neglected and the thermal conductivity approaches a T^2 dependence

$$K_g = (14.4k^3/h^2 v) T^2/(C+D) . \tag{14}$$

For the purpose of analyzing our data, Eq. (13) is written

$$K_g = \frac{2k^3 T^2}{v\hbar^2 (C+D)} \int_0^{\Theta/T} \frac{x^3 e^x\, dx}{(e^x - 1)^2 (1 + \alpha x^3 T^3)} , \tag{15}$$

$$\alpha = k^3 A/(C+D)\hbar^3 . \tag{16}$$

This equation was fit to the measured lattice thermal conductivities by selecting values of α and $(C+D)$ for each sample.

First an approximate value of the integral in Eq. (13) was obtained using the cutoff procedure suggested by Klemens,[16] namely,

$$K_g \approx \frac{2k^3 T^2}{v\hbar^2 (C+D)} \int_0^{x_c} \frac{x^3 e^x\, dx}{(e^x - 1)^2} = \frac{2k^3 T^2 J_3(x_c)}{v\hbar^2 (C+D)} , \tag{17}$$

where $x_c = 1/T\alpha^{1/3}$ and the J_3 values are tabulated.[17] The α which gave the best fit to experimental K_g/T^2 values was determined from the expression

$$\frac{100 K_g(T)}{T^2} = K_g(10\text{ K}) \left(\frac{J_3(1/T\alpha^{1/3})}{J_3(1/10\alpha^{1/3})}\right) , \tag{18}$$

using the experimental value of $K_g(10\text{ K})$. Since the $K_g(T)$ data approach a T^2 dependence at 10 K, Eq. (14) was used to approximate the sum of the scattering strengths $(C+D)$ from $K_g(10\text{ K})$. Finally, the point-defect scattering strength A was calculated from the values of $(C+D)$ and α. The scattering strengths A of the different Al-Mg alloys were found to scale with the alloy concentration f_0 as predicted by Eq. (12). This is a rapid and simple fitting procedure requiring only a desk calculator

TABLE II. Scattering parameters and values of the lattice thermal conductivity of the aluminum alloys. The parameter α is a measure of the ratio of the strength of the scattering of phonons by point defects to the sum of the strengths of the phonon scattering by electrons and dislocations [see Eq. (16)]. A describes the phonon scattering by point defects [see Eq. (12)] and f_0 is the atomic fraction of magnesium. K_g(10 K) is the smoothed value of the lattice thermal conductivity of each alloy at 10 K; K_g(1 K) is obtained by extrapolating Eq. (13) to 1 K using the above values of α and K_g(10 K) as described in the text. W_{gd} is the lattice thermal resistivity due to scattering of the phonons by dislocations; it is calculated from Eq. (22). N_d is the dislocation density calculated from Eq. (23). The absolute accuracy of the lattice thermal conductivity is ±5%. The error suggested by the listed values is indicative of the precision of the measurements.

Sample	$10^2 f_0$ (atomic fraction)	$10^7\ \alpha$ (K^{-3})	$10^{43} A$ (sec^3)	$10^{43} A/f_0$ (sec^3)	K_g(10 K) ($W\,m^{-1}\,K^{-1}$)	$10^2 K_g$(1 K) ($W\,m^{-1}\,K^{-1}$)	$10^{-2} W_{gd} T^2$ ($W^{-1}\,m\,K^3$)	$10^{-10} N_d$ (cm^{-2})
1	3.52	4.06	8.4	2.38	0.41	0.42	1.19	18
1a	•••	5.79	7.8	•••	0.62	0.65	0.37	5.7
1b	•••	7.51	8.2	•••	0.75	0.80	0.09	1
2a	4.00	5.79	7.6	1.89	0.64	0.67	0.33	5.1
2b	3.97	5.79	8.1	2.03	0.60	0.63	0.43	6.6
3	4.45	4.06	8.6	1.93	0.40	0.41	1.25	20
3a	4.06	5.79	7.7	1.89	0.63	0.66	0.36	5.5
3b	4.05	7.51	7.7	1.89	0.81	0.86	0.00	•••
4	6.11	11.66	11.9	1.94	0.79	0.86	0.00	•••
5	5.96	7.51	11.7	1.96	0.53	0.56	0.63	9.7
6	5.48	6.58	10.4	1.90	0.52	0.56	0.63	9.7
6a	5.27	7.51	9.9	1.88	0.62	0.66	0.36	5.5
7	5.13	7.51	9.8	1.90	0.64	0.68	0.31	4.8
8	•••	7.51	15.0	•••	0.35	0.37	1.53	23
9	•••	6.57	8.1	•••	0.67	0.71	0.24	3.7

and the tabulated J_3 integrals. In order to obtain more accurate values of α and $(C+D)$ a computer program was developed to numerically evaluate the integral in Eq. (15). Starting with the approximate values of α it was straightforward to find the value of α which gave the best fit to the K_g/T^2 data from 4 to 25 K, again using the experimental value of K_g(10 K). This type of fit is shown in Fig. 7, where the K_g/T^2 values for 4.1- and 6-at.%-Mg samples are plotted as a function of temperature. At temperatures above 25 K, the fits overestimate K_g as they should because Umklapp and normal processes are ignored. At temperatures below 10 K, K_g approaches a T^2 dependence as indicated by the gradual approach of the K_g/T^2 fits to a constant value at about 1 K as point defect scattering becomes negligible. The fits were extrapolated to obtain K_g(1 K) in order to obtain an accurate value of $(C+D)$ from Eq. (14). The values of K_g(1 K) and K_g(10 K) are listed in Table II for comparison. The latter values are not quite 100 times larger than the values of K_g(1 K) indicative of a small amount of point-defect scattering at 10 K.

The values of the point-defect scattering strength A calculated from α and $(C+D)$ are listed in Table II as well as A/f_0. The A values determined from our fitting procedure for the Al-Mg alloys were found to depend only on the magnesium concentration f_0 as expected. This is evident since these A values scale with f_0 such that A/f_0 has a constant value of $(1.9 \pm 0.1) \times 10^{-43}$ sec^3. The A/f_0 values were the same for both the heavily deformed and the well-annealed Al-Mg samples. This provides further evidence for the validity of our separation

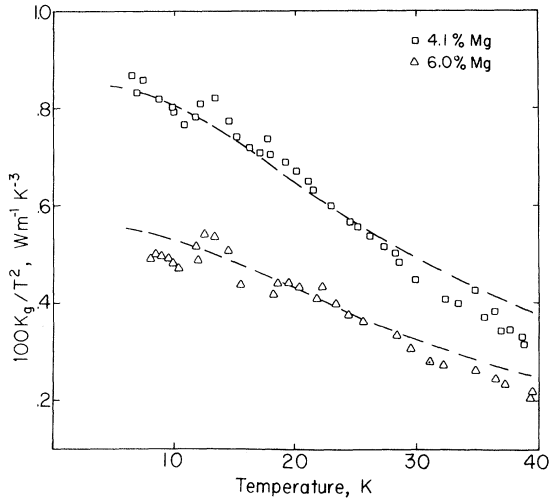

FIG. 7. Values of $100K_g/T^2$ vs absolute temperature T for samples 3b (4.1-at.% Mg) and 5 (6.0-at.% Mg). The curves are generated by numerical evaluation of the integral in Eq. (15) with the parameters given in Table II.

of the point-defect scattering and suggests that any non-equilibrium vacancy concentrations that might result from the cold working is very small.

Using Eq. (12), a value of $\Delta R/R = 0.046$ was calculated from the above A/f_0 value. This $\Delta R/R$ value is of the same order of magnitude as $\Delta a/(af_0) = 0.10$ (Ref. 18) for the change in the lattice constant of aluminum per atomic fraction of magnesium. Therefore, it seems reasonable to attribute the point defect scattering primarily to the local lattice distortion produced by a magnesium atom in aluminum.

The commercial 5052 and 2024 alloys contain solutes other than magnesium so their point defect scattering strengths A cannot be directly compared to those of the aluminum-magnesium alloys. However, in the case of the 5052 alloys the equivalent atomic fraction of magnesium f'_{Mg} required to give the same scattering as the nominal atomic fraction of chromium f_{Cr} (0.0012) of sample 1 was calculated using

$$f'_{\mathrm{Mg}} = \frac{(A/f_0)_{\mathrm{Cr}}}{(A/f_0)_{\mathrm{Mg}}} f_{\mathrm{Cr}} . \tag{19}$$

For consistency both the $\Delta a/(af_0)$ value for chromium (0.24) (Ref. 8) and for magnesium (0.1) were used for $\Delta R/R$ in Eq. (12) to calculate their respective A/f_0 values. In the case of chromium there was also a 6% contribution to A/f_0 from the mass difference between chromium and aluminum. The sum of f'_{Mg} (0.007) and the nominal magnesium concentration f_{Mg} (0.028) was then used to calculate an $A/(f'_{\mathrm{Mg}} + f_{\mathrm{Mg}})$ value of 2.38×10^{-43} for sample 1 which is listed in Table II. The rough agreement between this value and 1.9×10^{-43} for the Al-Mg alloys suggests that the scattering of phonons by Cr solutes can also be primarily accounted for in terms of the local lattice distortion. A value of A/f_0 for the annealed 5052 alloys is not listed because of the possibility of chromium precipitation during annealing. Similarly, a value of A/f_0 for the 2024 alloy is not included because the concentrations of magnesium, copper, and manganese remaining in solution after age hardening could not be determined.

The near equality of the values of K_g(1 K) for the samples annealed over 600 °C and slow cooled to about 400 °C before quenching suggests that for these samples dislocation-phonon scattering is negligible (i.e., $D = 0$). Since these are dilute alloys the lattice thermal conductivity of these samples ($K_g = 8.6\times10^{-3}T^2$ W m^{-1}K^{-1}) may be assumed to be that of pure aluminum. In this case only electron-phonon scattering is important and the above K_g expression might be compared to Klemens's calculation[1] which relates K_{ge} to W_i, namely,

$$K_{ge} = (313/W_i)\,(T/\Theta)^4\, N_a^{-4/3} . \tag{20}$$

N_a is the number of conduction electrons per atom (3) and $\Theta = 428$ K; the given value of the numerical coefficient depends on the assumption that the couplings between the electrons and the different phonon modes have equal strength. Using the values of W_i given in Eq. (6) one finds $K_{ge} = 0.97$ W m^{-1} K^{-1} at 10 K in excellent agreement with the experimental value. It is clear that if one were to use the empirical formula for W_i then the temperature dependence of K_{ge} would be $T^{2.1}$. Our experimental accuracy certainly does not permit any distinction between T^2 and $T^{2.1}$.

As is shown in Fig. 3 the K/T-vs-T plots extrapolate to a value of L/ρ_0 at $T = 0$. According to Pippard,[19] K_{ge} should contain an additional term linear in T when the electron mean free path is much shorter than the phonon wavelength. The wavelength λ_p of a typical phonon at a temperature T is of the order of $\Theta a/T$, where a is the lattice parameter. For example, λ_p has a value of about 40 nm at 4 K for aluminum. Using a free-electron model with three electrons per atom one obtains an electron mean free path of about 20 nm in an aluminum alloy of $\rho_0 = 2\times10^{-6}$ Ω cm. In the temperature range above 4 K one would not expect to observe this extra term since the values of λ_p/l_e are not sufficiently large. At lower temperatures the experimental error prevents any conclusion about the presence of this effect.

From the values of K_g(1 K), it is possible to estimate the dislocation density of the heavily swaged samples. At 1 K, the lattice thermal resistivity W_g is given by

$$W_g = K_g^{-1} = W_{ge} + W_{gd} , \tag{21}$$

where $W_{ge} = K_{ge}^{-1}$ is the thermal resistivity due to electron-phonon scattering and W_{gd} is the thermal resistivity due to dislocation-phonon scattering. Using the value of K_{ge} given above, W_{ge} is 116 m K W^{-1} at 1 K and for any sample containing dislocations

$$W_{gd}(1\ \mathrm{K}) = W_g(1\ \mathrm{K}) - 116 . \tag{22}$$

In Table II values of $W_{gd}T^2 = W_{gd}(1\ \mathrm{K})$ are listed for each sample. A value of N_d, the dislocation density, can be calculated from Ackermann's theoretical formula[15]

$$W_{gd}T^2 = 0.16K^2v\gamma^2b^2N_dh^2/k^3 , \tag{23}$$

where $b = \frac{1}{2}(\sqrt{2})\,a$ is the Burgers vector, $\gamma = 2.6$ (Ref. 20) is Grüneisen's constant and $v = 4.38\times10^5$ cm sec^{-1} is an average sound velocity.[21] Values of N_d so calculated are listed in Table II. According to this calculation the heavily swaged samples contain dislocation densities of about 2×10^{11} cm^{-2}.

The dislocation density can also be estimated from the expression recommended by Fickett[6] for

the residual resistivity increment due to dislocations:

$$(\Delta\rho_0)_d = (3\pm 1)\times 10^{-19} N_d\ \Omega\,\mathrm{cm}\ . \qquad (24)$$

The change in residual resistivity between the heavily swaged and well-annealed samples is $(9\pm1)\times10^{-8}$ Ω cm when there is no weight loss upon annealing. This change corresponds to a dislocation density of approximately 3×10^{11} cm^{-2} which is in reasonable agreement with the value of 2×10^{11} cm^{-2} considering that part of the change in residual resistivity may result from the migration of Mg atoms into grain boundaries or the formation of clusters. Because of the difficulties in counting dislocations in electron micrographs of heavily deformed metals and the uncertainties in the electrical resistivities, it seems to us that the measurements of the lattice thermal conductivity provide a superior tool for the study of dislocations in heavily deformed alloys.

There are several samples whose K_g values suggest the presence of additional scattering mechanisms. The first is sample 2, whose lattice thermal conductivity was measured after an anneal and a quench at 465 °C (sample 2a), and after an anneal at 500 °C followed by a slow cool to 200 °C (sample 2b). The K_g(10 K) value of sample 2b is less than that of sample 2a as shown in Table I. The fact that K_g(10 K) of the slow-cooled sample is not larger than that of the quenched sample certainly shows that quenching from 400 °C does not introduce a significant number of dislocations. The decrease in K_g(10 K) for the slow-cooled sample might result from the formation of solute atmospheres[22] around the dislocations remaining after the 500 °C anneal.

Another sample with an unusual behavior is sample 9 which was annealed at 609 °C and quenched from 567 °C in order to ensure that its Cr remained in solution. All of our other samples were quenched from temperatures below 400 °C. In Fig. 5 the lattice thermal conductivity of the 5052 samples 1 and 9 are plotted as a function of temperature for the sake of comparison. Both sample 1 in its various stages of heat treatment and sample 9 display the T^2 dependence below 10 K expected from sessile dislocation-phonon scattering and electron-phonon scattering. However, the K_g values of sample 9 are significantly reduced from those of sample 1b which was also annealed above 600 °C. This result is difficult to explain at present. Previous electron microscopy studies on aluminum specimens[12] and a 1.5-at.%-Mg alloy[23] indicate the dislocation loop densities from 10^{13} to 10^{14} cm^{-3} with average loop diameters of 10 to 100 nm are obtained when quenching from temperatures above 530 °C. These concentrations and loop sizes correspond to dislocation densities of approximately 10^9 cm^{-2}. However, a sessile dislocation density of about 4×10^{10} cm^{-2} is required to explain the differences in the values of the lattice thermal conductivity of samples 1b and 9.

Recently, O'Hara and Anderson[24] reported measurements of the thermal conductivity of pure aluminum at temperatures below 1 K. They showed that their results might be understood if the phonons were scattered by vibrating dislocations. If this scattering mechanism were also to be important at higher temperatures the scattering strength per dislocation would be much larger. Any attempt to associate the behavior of sample 9 with such phenomena is at present highly speculative and will require further measurements.

V. CONCLUSIONS

An analysis of the lattice thermal conductivity of a number of aluminum-magnesium alloys has separated the effects of the electron-phonon, dislocation-phonon, and point-defect–phonon scattering. The following conclusions summarize this work.

(i) The lattice thermal conductivity of pure defect-free aluminum in the temperature range where phonons are scattered only by electrons (roughly below 20 K) is given by $K_g = 8.6\times10^{-3}T^2$ W m^{-1} K^{-1} in good agreement with theory.

(ii) The lattice thermal resistivity due to phonon scattering by dislocations in the temperature range 4–25 K varies as T^{-2} characteristic of scattering by sessile dislocations.

(iii) Dislocation densities of about 2×10^{11} lines cm^{-2} are introduced by heavy swaging. This number is consistent with electron microscopy and is probably more reliable than that estimated from a count of a mass of dislocation tangles.

(iv) The point-defect scattering scales with the solute concentration and for the most part appears to be the result of a local distortion of the lattice (~5%) produced by the introduction of the magnesium atoms.

(v) Changes in the lattice thermal conductivity caused by various heat treatments have been observed. They may be associated with the formation of solute atmospheres and/or quenched in dislocation loops.

ACKNOWLEDGMENTS

The authors gratefully acknowledge the assistance of Larry McCurdy in using the electron microscope. Conversations with Dr. P. G. Klemens were most helpful. Helium gas was supplied by the U. S. Office of Naval Research under Contract No. 4500/N0014-71-0-0249. The data analysis was performed at the University of Connecticut Computer Center under NSF Grant No. GJ-9.

†Supported by the U. S. Air Force Office of Scientific Research under Grant No. AFOSR-73-2418.

*Present address: Brookhaven National Laboratory, Upton, N. Y. 11973.

[1]P. G. Klemens, Solid State Phys. 7, 1 (1958).

[2]R. Powell, W. Hall, and H. Roder, J. Appl. Phys. 31, 496 (1960).

[3]P. Täubert, F. Thom, and U. Gammert, Cryogenics 13, 149 (1973).

[4]R. Klaffky, N. S. Mohan, and D. H. Damon, Proceedings of the Thirteenth International Thermal Conductivity Conference (unpublished).

[5]D. K. Chatterjee and K. M. Entwistle, J. Inst. Metals 101, 53 (1973).

[6]F. R. Fickett, Cryogenics 11, 349 (1971).

[7]M. C. Karamargin, C. A. Reynolds, F. P. Lipschultz, and P. G. Klemens, Phys. Rev. B 5, 2856 (1972).

[8]J. G. Hust and L. L. Sparks, NBS Report No. 9790, U. S. Natl. Bur. Stds. Inst. Basic Studies, Boulder, Colo.

[9]R. W. Klaffky, N. S. Mohan, and D. H. Damon (unpublished).

[10]E. W. Fenton, J. S. Rogers, and S. B. Woods, Can. J. Phys. 41, 2026 (1963).

[11]Y. S. Touloukian, R. W. Powell, C. Y. Ho, and P. G. Klemens, *Thermophysical Properties of Matter* (Plenum, New York, 1970).

[12]R. P. Reed, Cryogenics 12, 259 (1972).

[13]N. S. Mohan, R. W. Klaffky, L. C. Harrington, and D. H. Damon, I.M.S. Special Report TPROP 1, "The Thermal Conductivity of some Aluminum Alloys between 5 and 60 K."

[14]P. G. Klemens, in *Handbuch der Physik*, edited by S. Flügge (Springer, Berlin, 1956), Vol. 14, p. 198.

[15]M. W. Ackerman, Phys. Rev. B 5, 2751 (1972).

[16]P. G. Klemens, Proc. R. Soc. A 208, 108 (1951).

[17]W. M. Rogers and R. L. Powell, *Tables of Transport Integrals*, U. S. Natl. Bur. Stds. Inst. Circ. No. 595 (U. S. GPO, Washington, D. C., 1958).

[18]W. B. Pearson, *Lattice Spacings and Structures of Metals and Alloys* (Pergamon, Oxford, 1958).

[19]A. B. Pippard, Philos. Mag. 46, 1104 (1955).

[20]J. G. Collins and G. K. White, in *Progress in Low Temperature Physics*, edited by G. J. Gorter (North-Holland, Amsterdam, 1964), Vol. 4, p. 450.

[21]G. N. Kamm and G. A. Alers, J. Appl. Phys. 34, 327 (1964).

[22]M. A. Mitchell, P. G. Klemens, and C. A. Reynolds, Phys. Rev. B 3, 1119 (1971).

[23]V. N. Rozhanskii, V. V. Kirichenko, and V. V. Slezov, Fiz. Tverd. Tela 15, 349 (1973) [Sov. Phys.-Solid State 15, 258 (1973)].

[24]S. G. O'Hara and A. C. Anderson, Phys. Rev. B 9, 3730 (1974).